

Exploring Solid-State Nanopore Approach for Single-Molecule Protein Detection from Single Cells

Zi-Qi Zhou^a, Shao-Chuang Liu^{*a}, Jia Wang^a, Ke-Le Chen^a, Bao-Kang Xie^a, Yi-Lun Ying^{a, b}, Yi-Tao Long^{*a}

a. Molecular Sensing and Imaging Center, School of Chemistry and Chemical Engineering, Nanjing University, Nanjing, 210023, P.R. China.

b. Chemistry and Biomedicine Innovation Center, Nanjing University, Nanjing, 210023, P.R. China.

Email: yitaolong@nju.edu.cn, shaochuanliu@nju.edu.cn

Abstract: Direct protein analysis from complex cellular samples is crucial for understanding cellular diversity and disease mechanisms. Here, we explored the potential of SiN_x solid-state nanopores for single-molecule protein analysis from complex cellular samples. Using the LOV2 protein as model, we designed a nanopore electrophoretic driver protein and fused it with LOV2, thereby enhancing the capture efficiency of the target protein. Then, we performed ex-situ single-cell protein analysis by directly extracting the contents of individual cells using the glass nanopipette-based single-cell extraction and successfully identified and monitored the conformational changes of the LOV2 protein from single-cell extracts using SiN_x nanopores. Our results reveal significant differences between proteins measured directly from single cells and those obtained from purified samples. This work demonstrates the potential of solid-state nanopores as a powerful tool for single-cell, single-molecule protein analysis, opening avenues for investigating protein dynamics and interactions at the cellular level.

Context

Methods and reagents	1
Data supplementation	6
Figure S1. Fluorescent characterization of cells after transfection of plasmids and fluorescent characterization of purified proteins.	6
Figure S2. Additional raw current trace of CL-293T, CL-LOV2-293T and CL-NEPD-LOV2-293T in figure 1f.....	7
Figure S3. Additional raw current trace of NEPD and NEPD-LOV2 in figure 2a	8
Figure S4. Supplemented data analysis of purified NEPD protein samples using 5.7nm-in-diameter solid-state nanopore	9
Figure S5. Supplemented data analysis of purified NEPD protein samples using 8.4nm-in-diameter solid-state nanopore	10
Figure S6. Supplemented data analysis of purified NEPD protein samples using nm 3.57 nm - 6.73 nm diameter solid-state nanopore.	11
Figure S7. Supplemented data analysis of purified NEPD and NEPD-LOV2 protein samples using 5.0nm-in-diameter solid-state nanopore	12
Figure S8. Supplemented light experiment analysis of purified NEPD-LOV2 protein samples using 9.0nm-in-diameter solid-state nanopore.....	13

Figure S9. Identification of target protein in cell lysate samples	14
Figure S11. Supplemented data analysis of CL-NEPD using 12nm-in-diameter solid-state nanopore	15
Figure S12. Supplemented data analysis of CL-NEPD using 6nm-in-diameter solid-state nanopore.....	16
Figure S13. Supplemented data analysis of CL-NEPD-LOV2 using 6 nm-in-diameter solid-state nanopore.	17
Figure S14. Supplemented data analysis of CL-NEPD-LOV2 using 6 nm-in-diameter solid-state nanopore.	18
Figure S15. Additional raw current trace of 293T, NEPD-LOV2-293T and NEPD-LOV2-293T + NEPD-LOV2 in figure 3	19
Figure S16. Supplemented data analysis of 293T using 6nm-in-diameter solid-state nanopore.	20
Figure S17. Supplemented data analysis of NEPD-LOV2-293T using 6nm-in-diameter solid-state nanopore ...	21
Figure S18. Additional raw current trace of NEPD-LOV2-293T and NEPD-LOV2-293T + NEPD-LOV2 with light condition in fig 4.	22

Methods and reagents

Reagents and chemicals

293T cells were purchased from Aladdin Chemistry Co. Ltd. (Shanghai, China). KCl ($\geq 99\%$), Tris(hydroxymethyl)aminomethane (Tris, $\geq 99\%$), Imidazole ($\geq 99\%$) and $\text{Na}_3\text{PO}_4 \cdot 12\text{H}_2\text{O}$ ($\geq 98\%$) were all purchased from Sigma-Aldrich Co. RIPA Lysis Buffer (Moderate) was purchased from Beyotime (Shanghai, China). NaCl (AR, 99.5%) was purchased from MACKLIN (Shanghai, China). DMEM basic (1X), Premium Plus FBS, Trypsin-EDTA (1X, 0.05%), PBS Buffer (1X), Pen Strep were all purchased from Gibco (Shanghai, China). PEI was purchased from BIOHUB (Shanghai, China). Ni Sepharose excel was purchased from Cytiva (Shanghai, China). PMSF (100 mM) was purchased from Biosharp (Beijing, China).

All solutions were prepared using ultrapure water (18.2 M Ω cm at 25 °C) from a Milli-Q system (Billerica, MA, USA).

Plasmid construction, protein expression purification and quantitative characterization.

The blue light-sensing light-oxygen-voltage2 (LOV2) were human codon-optimized and synthesized by Genewiz. EGFP was a gift from Dali Li (East China Normal University). Oligonucleotides encoding of the peptides (NEPD and NEPD-LOV2) or linkers were introduced using primers through PCR. DNA fragments were amplified using KOD-Plus-Neo DNA polymerase (Toyobo, KOD-401) and assembled by ClonExpress MultiS One Step Cloning Kit (Vazyme). The DNA cassettes of LOV2, EGFP, EGFP-LOV2 were cloned into the transposon-bearing plasmid pT2/BH (Addgene #26557) under the control of CMV promoter, respectively. All plasmids used in this study were constructed using standard molecular biology techniques and confirmed by Sanger sequencing (Tsingke Biotechnology Co., Ltd).

We introduced the synthesized plasmid into 293T cells for expression. The plasmid was mixed with the transfection reagent polyethylenimine (PEI) in a 1:3 ratio (DNA:PEI) in DMEM without serum. The mixture was incubated at room temperature for 15 minutes and then added to the culture dish containing 293T cells. After 8 hours, the medium was changed to fresh DMEM. Transfection efficiency was monitored over time, and the maximum efficiency was achieved after 48 hours. To prepare the cell sample, the transfected cells were lyophilized at -54°C . For the preparation of the pure protein sample, a His-tag was ligated to the model protein.

The supernatant was then purified using a nickel affinity column, eluting the protein with 300 mM imidazole.

Nanopore fabrication and characterization

The solid-state nanopores were fabricated by controlled dielectric breakdown. Free-standing SiN film with thickness of 12 nm supported on a silicon frame (Norcada, Canada, NBPT005Z-HR) was mounted in a liquid cell, separating two reservoirs with 1M KCl buffered to pH 10 with 10mM Tris-HCl and 1mM EDTA as electrolyte. The bias voltage across the membrane was applied via a pair of Ag/AgCl electrodes connected to a home-build circuit, controlled by analogue data acquisition board (PCI-6251, National Instruments). The breakdown voltage was set constantly with a typical value as 8 V, which would be adjusted according the leakage current. The leakage current under 8 V with our experimental condition is typically 10-50 nA. A threshold of current was set according to the expected nanopore size, estimated by the pore conductance based on a cylindrical pore model, as Equation S1.

$$G = \sigma \left[\frac{4l}{\pi d^2} + \frac{1}{d} \right]^{-1} \quad (1)$$

A rapid current increase caused by the breakdown event could be observed, indicates the initial formation of the nanopore. After the breakdown, we hold the DC voltage which induce the continuously increasing of the ionic current, indicates the enlargement of the nanopore, until the current reach the set threshold. Once the nanopore with desired pore size is obtained, the home-build circuit would be replaced by a commercial low-current amplifier (Axopatch 200B, Molecular Devices, US) then the open pore current under experimental bias voltages and the I-V curve could be measured. If the open pore current was stable under experimental potential and the I-V curve was linear, the nanopore could be used for the further experiments. Otherwise, following procedures would be applied to improve the nanopore condition: 1) replace the electrolyte into 4M LiCl and soak the whole device in the 1M LiCl solution overnight (>12 h) if the open pore current is not stable or the Root-Mean-Square (RMS) of open pore current is larger than tolerance (200 pA under 10 kHz bandwidth typically) or the I-V curve is asymmetry and linear; 2) apply a square wave voltage pulse to enlarge the nanopore till the expected nanopore size is reached. It should be noticed that in some cases, after the treatments mentioned above, the quality of certain nanopore devices might still cannot meet the requirement of the experiments. In this case, those nanopore chips will not be used for the further experiments. The final pore size would be estimated by the conductance measurement based on Equation 1. We also noticed that the fabrication time, noise level of nanopores, and success rate of controlled dielectric breakdown, under our

experimental condition highly affected by the quality of SiNx membrane and a difference between batches is obviously existed.

Identification of target protein in cell lysate samples

To identify target protein signals within cellular samples, we introduced purified proteins during the analysis of cell lysate samples. Initially, we measured the cell lysate samples at the voltages of range from + 100 mV to 200 mV using a nanopore with diameter about 5.61 nm. Following this, we added purified protein to the same nanopore and continued signal collection. Figure S9 show the representative current traces and individual events from the cell lysate expressing NEPD protein, along with the signals obtained after adding purified NEPD protein. After adding the purified protein, we observed a slight increase in the signal capture rate. The scatter plot in figure S9b reveals significant overlap in signal distributions at each voltage, suggesting that the signals obtained from the cell lysate primarily originate from the NEPD tag protein. Its unique charge and structural properties enhance its capture efficacy by the nanopore. Statistical analysis indicates that the blockage current distribution shifted only slightly after adding the purified protein at + 100 mV, + 150 mV and + 200 mV, respectively (Fig. S9b). By comparing the differences between the two distributions, the signal of the target protein within the cell lysate sample can be confirmed.

Then, we applied the same method to analyze cell lysates expressing NEPD-LOV2 proteins. Figure S9c show the representative current traces and individual events at the voltages of range from + 200 mV to 300 mV using a nanopore with diameter 5.61 nm. Similar to the NEPD protein, a slight increase in the signal capture rate was observed after adding purified NEPD-LOV2 protein. However, the signal distributions before and after the addition of purified protein showed significant overlap (Fig. S9d). This indicates that the signal obtained from the cell lysate primarily corresponds to the NEPD -LOV2 protein. In Supplementary Figures S10 - S13, we present additional data on cell lysate measurements using the nanopore of different size. Our findings indicate that measuring complex cell lysate samples faces more challenging than measuring purified proteins. Two significant issues arose during the measurement of cell samples: firstly, the nanopore's diameter tends to gradually increase over time, limiting the duration of stable measurements; secondly, the complex cellular contents often block the nanopore channel. These factors significantly affect the quality and consistency of the measured signals.

Single-cell extraction.

Experiments on single-cell manipulation were performed with a micromanipulator, which was integrated on a Nikon Ti-2 microscope and a pico-pump (model LPP01-100). Adjust the position of the micromanipulator to align the nanopipette with the target cell. Using the micromanipulation system, the nanopipette was moved under a 10x objective lens to locate the focal plane of the nanopipette tip. The nanopipette was then gradually lowered until its tip penetrated the cell membrane under a 40x objective lens. The successful insertion of the nanopipette into the cell was verified by observing that the cell moved in response to horizontal movements of the nanopipette. After inserting the nanopipette into the cell, a pico-pump was used to aspirate a portion of the cellular content for approximately 5 seconds. The nanopipette was then retracted from the cell and quickly inserted into the detection chamber.

Data supplementation

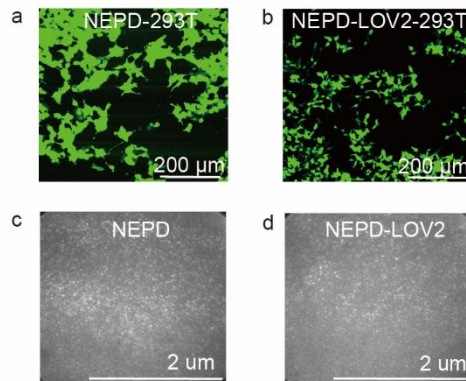


Figure S1 Fluorescent characterization of cells after transfection of plasmids and fluorescent characterization of purified proteins.

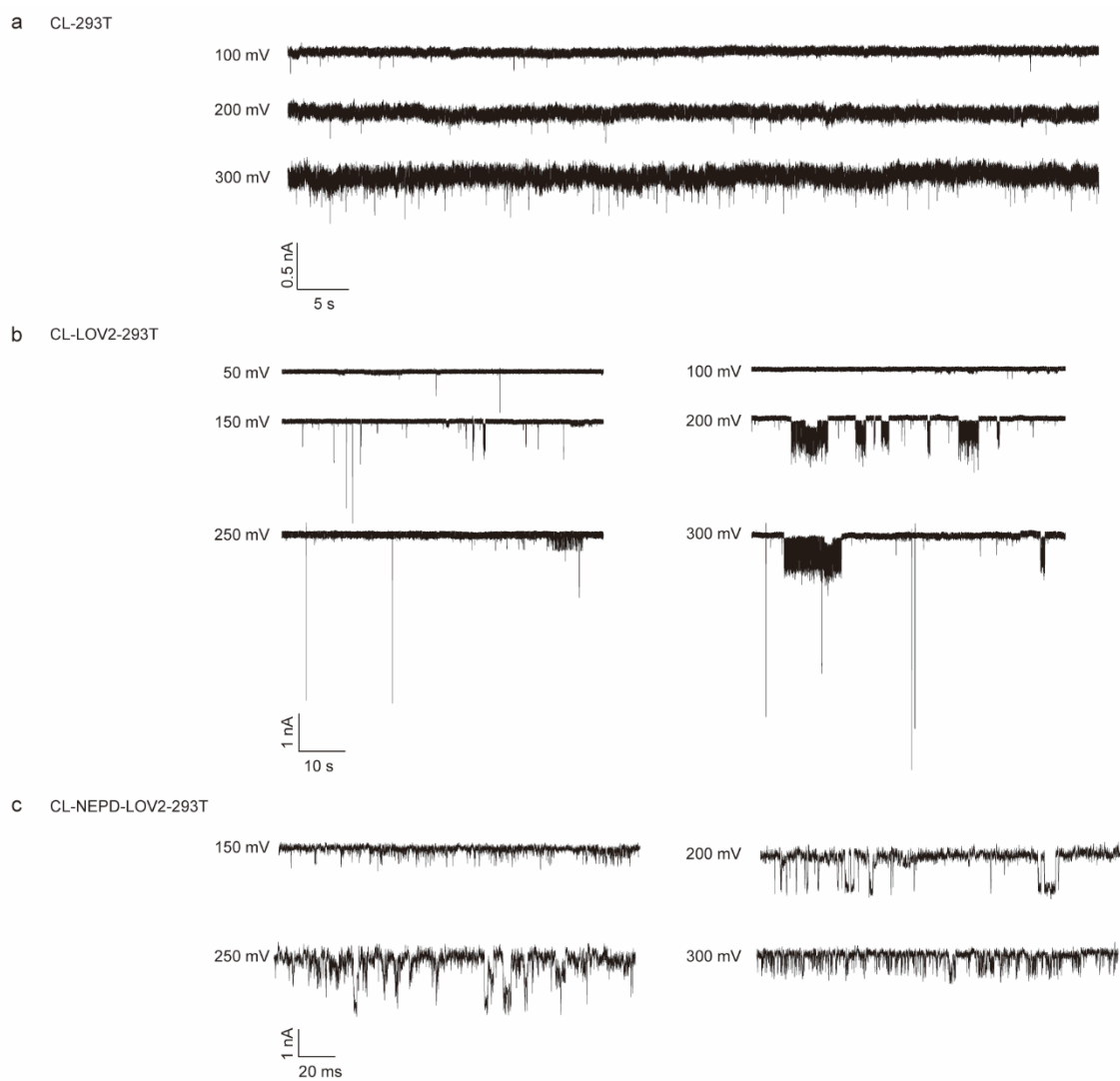


Figure S2. Additional raw current trace of CL-293T, CL-LOV2-293T and CL-NEPD-LOV2-293T in fig 1f. (a) The raw current trace of CL-293T at 100 mV, 200 mV and 300 mV. (b) The raw current trace of CL-LOV2-293T at 50mV, 100 mV, 150mV, 200 mV ,250 mV and 300 mV. (a) The raw current trace of CL-NEPD-LOV2-293T at 100 mV, 200 mV and 300 mV. All the data was acquired in 1 M KCl, 10 mM Tris-HCl, 1 mM EDTA, pH 7.40. All data is recorded with a sample rate of 100 kHz and filtered at 10 kHz.



Figure S3. Additional raw current trace of NEPD and NEPD-LOV2 in figure 2a. All the data was acquired in 1 M KCl, 10 mM Tris-HCl, 1 mM EDTA, pH 7.40. All data is recorded with a sample rate of 100 kHz and filtered at 10 kHz.

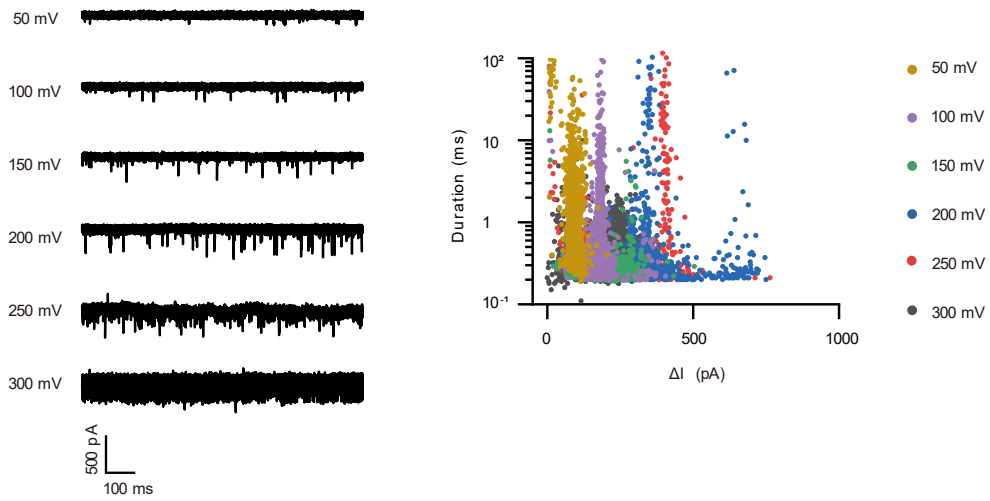


Figure S4. Supplemented data analysis of purified NEPD protein samples using 5.7nm-in-diameter solid-state nanopore. The raw current trace of NEPD under different bias (left). Scatter plots for duration vs ΔI (right). Yellow: 50 mV (959), purple: 100 mV (1027), green: 150 mV (994), blue: 200 mV (1359), Red: 250 mV (1382), and grey: 300 mV (1088).



Figure S5. Supplemented data analysis of purified NEPD protein samples using 8.4nm-in-diameter solid-state nanopore. (a)The raw current trace of NEPD-LOV2 at 300mV voltage. (b) Scatter plots for duration vs ΔI (right). Point: 272. All the data was acquired in 1 M KCl, 10 mM Tris-HCl, 1 mM EDTA, pH 7.40. All data is recorded with a sample rate of 100 kHz and filtered at 10 kHz.

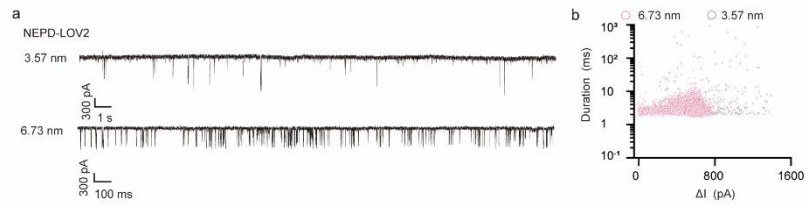


Figure S6. Supplemented data analysis of purified NEPD protein samples using 3.57 nm - 6.73 nm diameter solid-state nanopore. (a) The raw current trace of NEPD-LOV2 at 300mV voltage. (b) Scatter plots for duration vs ΔI . Pink: 6.73 nm (3446) and grey: 3.57 nm (272). All the data was acquired in 1 M KCl, 10 mM Tris-HCl, 1 mM EDTA, pH 7.40. All data is recorded with a sample rate of 100 kHz and filtered at 10 kHz.

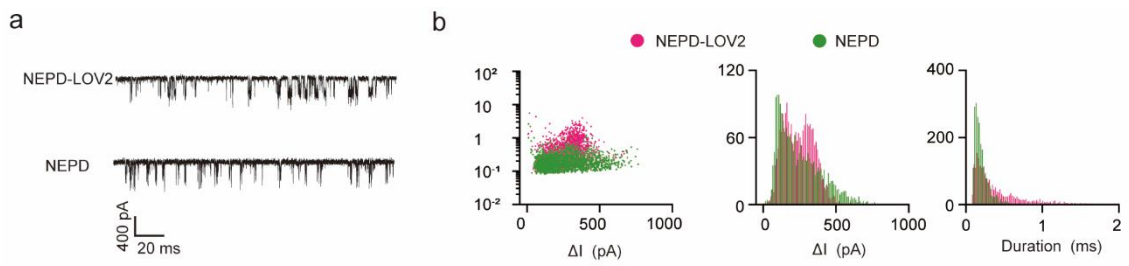


Figure S7. Supplemented data analysis of purified NEPD and NEPD-LOV2 protein samples using 5.0nm-in-diameter solid-state nanopore. (a) The raw current trace of NEPD-LOV2 and NEPD at 300mV voltage. (b) The statistics results that the scatter plots for duration vs ΔI , histogram of the ionic current blockades and histogram of the duration blockades for purified NEPD and NEPD-LOV2 protein samples in 5.0nm-in-diameter solid-state nanopore at 300 mV. Pink: NEPD-LOV2 (2176) and green: NEPD (2176). All the data was acquired in 1 M KCl, 10 mM Tris-HCl, 1 mM EDTA, pH 7.40. All data is recorded with a sample rate of 100 kHz and filtered at 10 kHz.

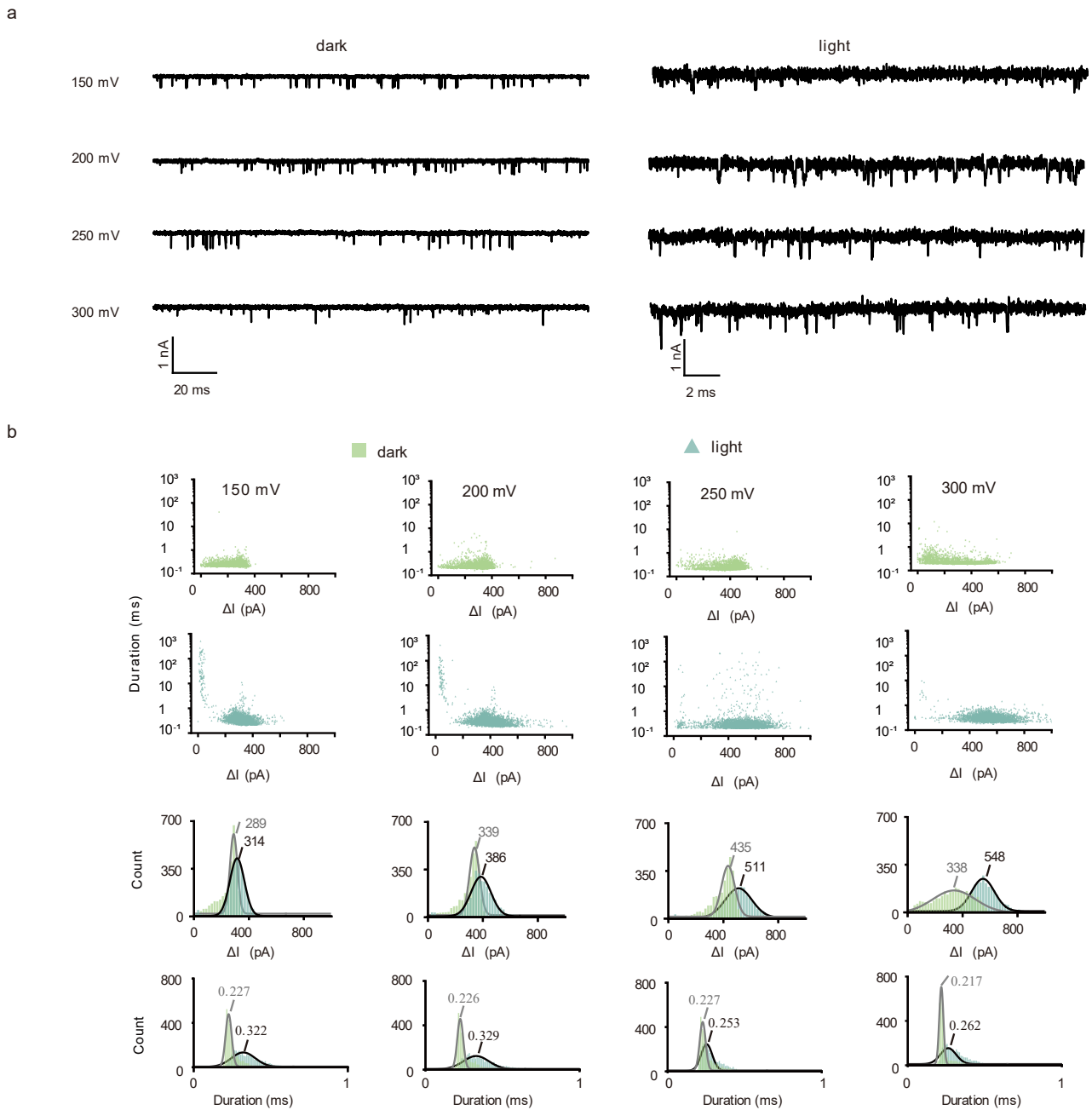


Figure S8. Supplemented light experiment analysis of purified NEPD-LOV2 protein samples using 9.0nm-in-diameter solid-state nanopore. (a) The raw current trace of NEPD-LOV2 at 150mV, 200mV, 250mV and 300mV voltage. (b) The statistics results of duration vs ΔI , histogram of the ionic current blockades and histogram of the duration blockades for purified NEPD-LOV2 protein samples at 150mV, 200mV, 250mV and 300mV voltage. All the points are 3000.

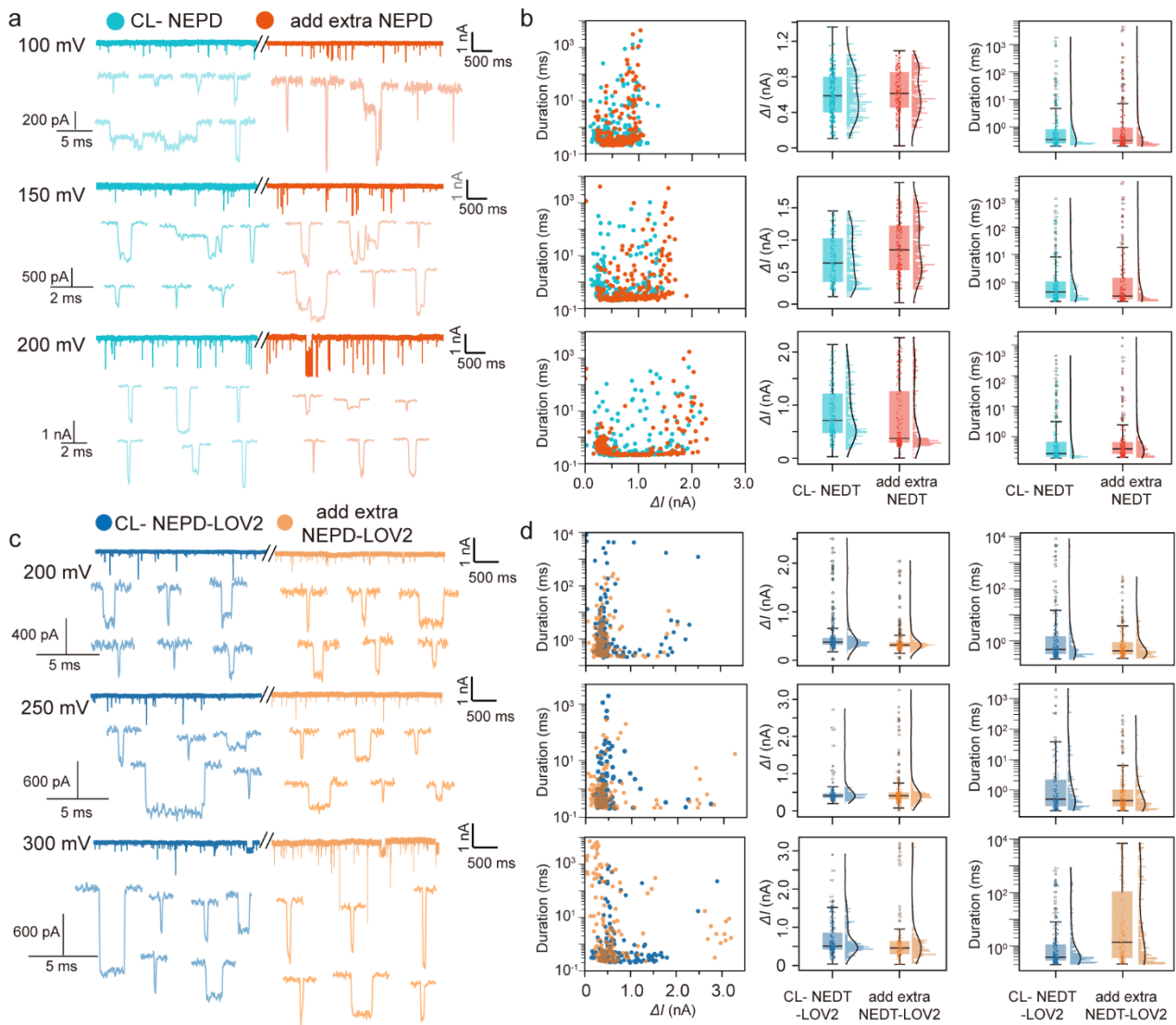


Figure S9. (a) The representative current trace and individual example events of cell lysate expressing NEPD protein, along with the signals obtained after adding purified NEPD protein at the voltages of range from + 100 mV to 200 mV using a 5.61 nm nanopore. (b) Scatter plots of blockage current versus dwell time (N=222), and corresponding box with strip plots of blockage current and dwell time, along with the histogram distribution. (c) The representative current trace and individual example events of cell lysate expressing NEPD-LOV2 protein, along with the signals obtained after additional purified NEPD-LOV2 proteins added at the voltages of range from + 200 mV to 300 mV using a 5.61 nm nanopore. (d) Scatter plots of blockage current versus dwell time (N=222), and corresponding box with strip plots of blockage current and dwell time, along with the histogram distribution.

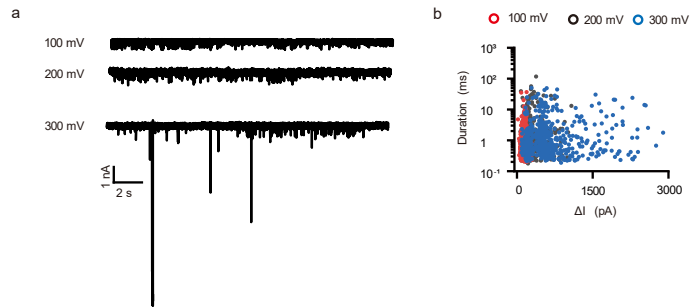


Figure S10. Supplemented data analysis of CL-NEPD using 12nm-in-diameter solid-state nanopore. (a) The raw current trace of CL-NEPD at 100mV, 200mV and 300mV voltage. (b) Scatter plots for duration vs ΔI at 100mV, 200mV and 300mV voltage. Red: 100 mV (1616), black: 200 mV (516) and green: 300 mV (547). All the data was acquired in 1 M KCl, 10 mM Tris-HCl, 1 mM EDTA, pH = 7.40. All data is recorded with a sample rate of 100 kHz and filtered at 10 kHz.

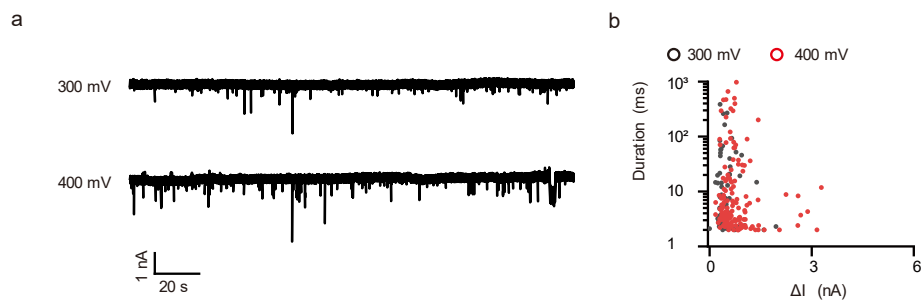


Figure S11. Supplemented data analysis of CL-NEPD using 6nm-in-diameter solid-state nanopore. (a) The raw current trace of CL-NEPD at 300mV, 400mV voltage. (b) Scatter plots for duration vs ΔI at 300 mV and 400 mV. Black: 300 mV (73) and red: 400 mV (156). All the data was acquired in 1 M KCl, 10 mM Tris-HCl, 1 mM EDTA, pH = 7.40 and recorded with a sample rate of 10 kHz and filtered at 10 kHz.

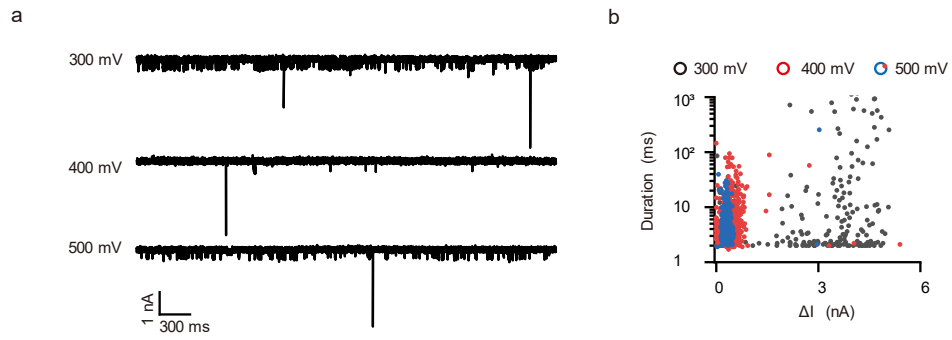


Figure S12. Supplemented data analysis of CL-NEPD-LOV2 using 6nm-in-diameter solid-state nanopore. (a) The raw current trace of CL-NEPD-LOV2 at 300mV, 400mV and 500mV voltage. (b) Scatter plots for duration vs ΔI at 300mV, 400mV and 500mV voltage. Black: 300 mV (1761), Red: 400 mV (4080) and blue: 500 mV (1518). All the data was acquired in 1 M KCl, 10 mM Tris-HCl, 1 mM EDTA, pH = 7.40 and recorded with a sample rate of 10 kHz and filtered at 10 kHz.

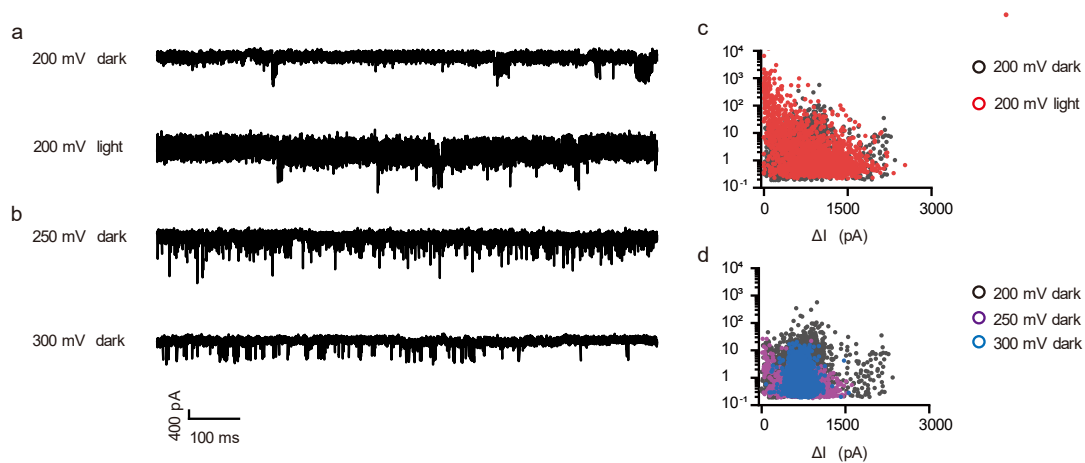


Figure S13. Supplemented data analysis of CL-NEPD-LOV2 using 6nm-in-diameter solid-state nanopore. (a) The raw current trace of CL-NEPD-LOV2 at 200mV under dark and blue light condition. (b) Scatter plots for duration vs ΔI at 200mV under dark and blue light on condition. Black: dark (3756) and Red: light (1654). (c) The raw current trace of CL-NEPD-LOV2 at 250mV and 300 mV under dark condition. (d) Scatter plots for duration vs ΔI at 200 mV, 250mV and 300mV voltage. Black: 200 mV (1761), Purple: 300 mV (4080) and blue: 300 mV (1518). All the data was acquired in 1 M KCl, 10 mM Tris-HCl, 1 mM EDTA, pH = 7.40 and recorded with a sample rate of 100 kHz and filtered at 10 kHz.

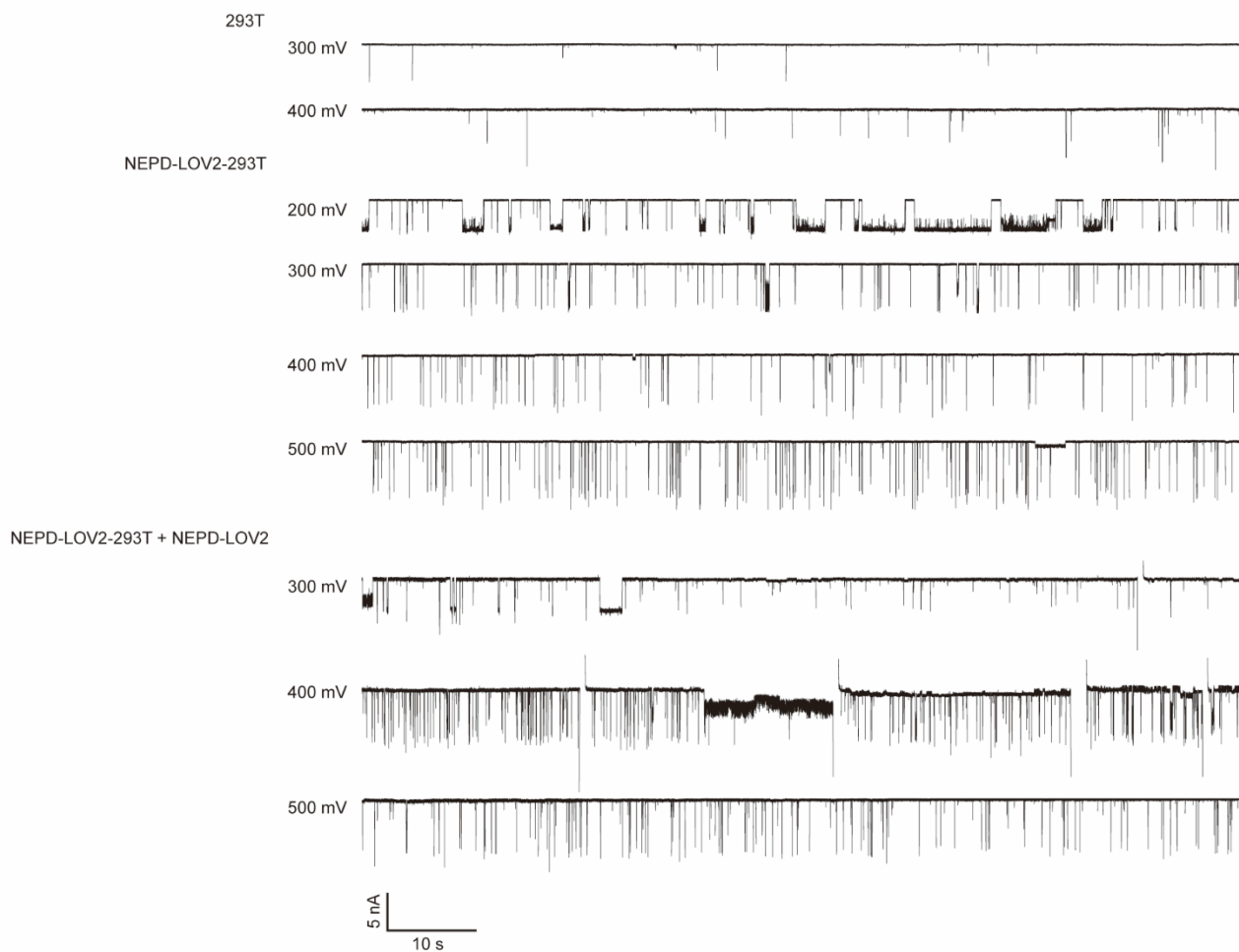


Figure S14. Additional raw current trace of 293T, NEPD-LOV2-293T and NEPD-LOV2-293T + NEPD-LOV2 in figure 3. The raw current trace of 293T at 300mV and 400mV voltage, using 9nm-in-diameter solid-state nanopore. The raw current trace of NEPD-LOV2-293T at 200mV, 300mV, 400mV and 500mV voltage, using 8nm-in-diameter solid-state nanopore. The raw current trace of NEPD-LOV2-293T + NEPD-LOV2 at 300mV, 400mV and 500mV voltage, using 8nm-in-diameter solid-state nanopore. All the data was acquired in 1 M KCl, 10 mM Tris-HCl, 1 mM EDTA, pH = 7.40 and recorded with a sample rate of 100 kHz and filtered at 10 kHz.

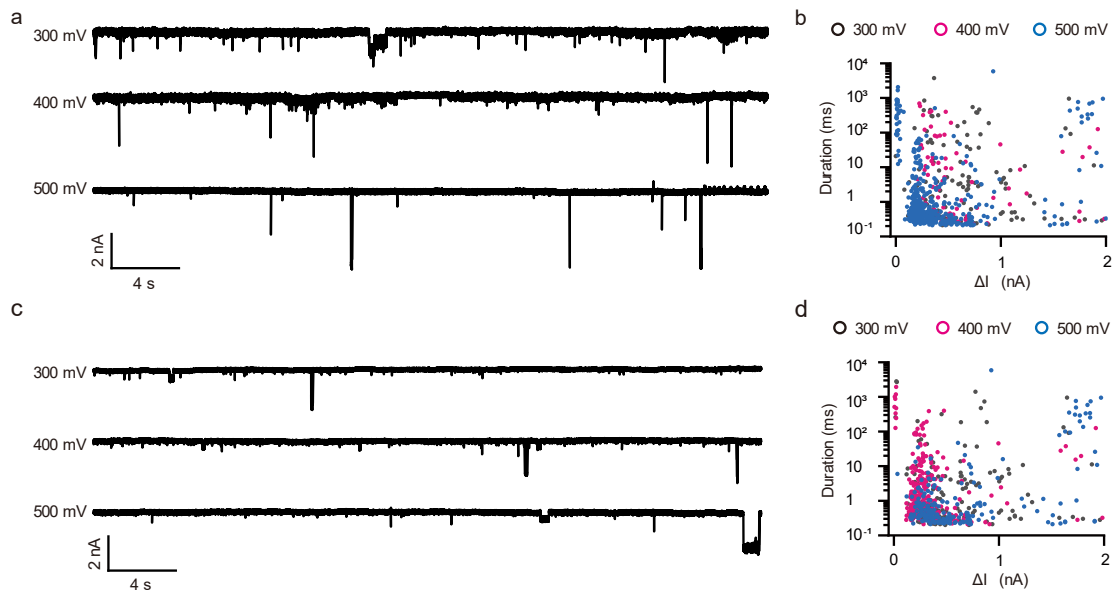


Figure S15. Supplemented data analysis of 293T using 6nm-in-diameter solid-state nanopore. (a) The raw current trace of 293T at 300mV, 400mV and 500mV voltage, using 6nm-in-diameter solid-state nanopore. (b) Scatter plots for duration vs ΔI . Black: 300 mV (152), Red: 400 mV (80) and blue: 500 mV (549). (c) The raw current trace of 293T at 300mV, 400mV and 500mV voltage, using 6nm-in-diameter solid-state nanopore. (d) Scatter plots for duration vs ΔI . Black: 300 mV (212), Red: 400 mV (281) and blue: 500 mV (225).

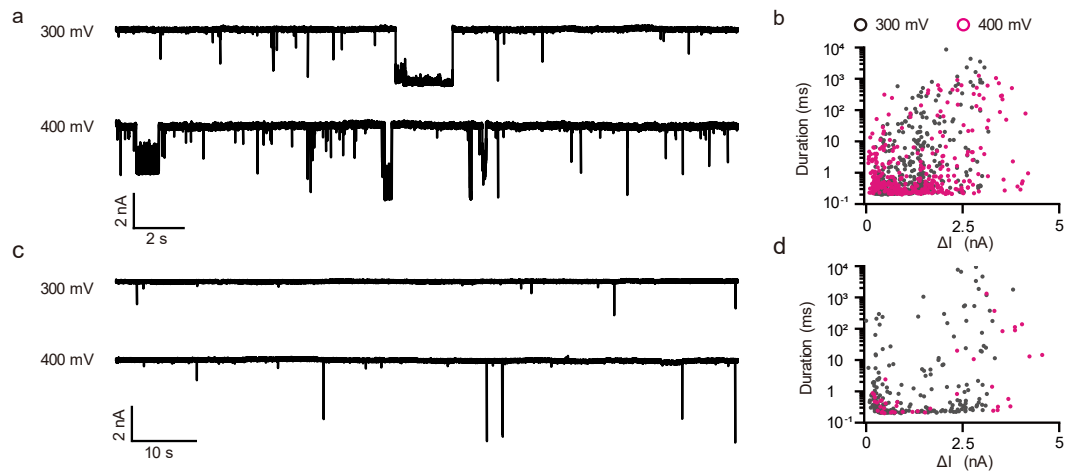


Figure S16. Supplemented data analysis of NEPD-LOV2-293T using 6nm-in-diameter solid-state nanopore. (a) The raw current trace of 293T at 300mV, 400mV and 500mV voltage, using 6nm-in-diameter solid-state nanopore. (b) Scatter plots for duration vs ΔI . Black: 300 mV (423) and Red: 400 mV (375). (c) The raw current trace of 293T at 300mV, 400mV and 500mV voltage, using 6nm-in-diameter solid-state nanopore. (d) Scatter plots for duration vs ΔI . Black: 300 mV (247) and Red: 400 mV (42).

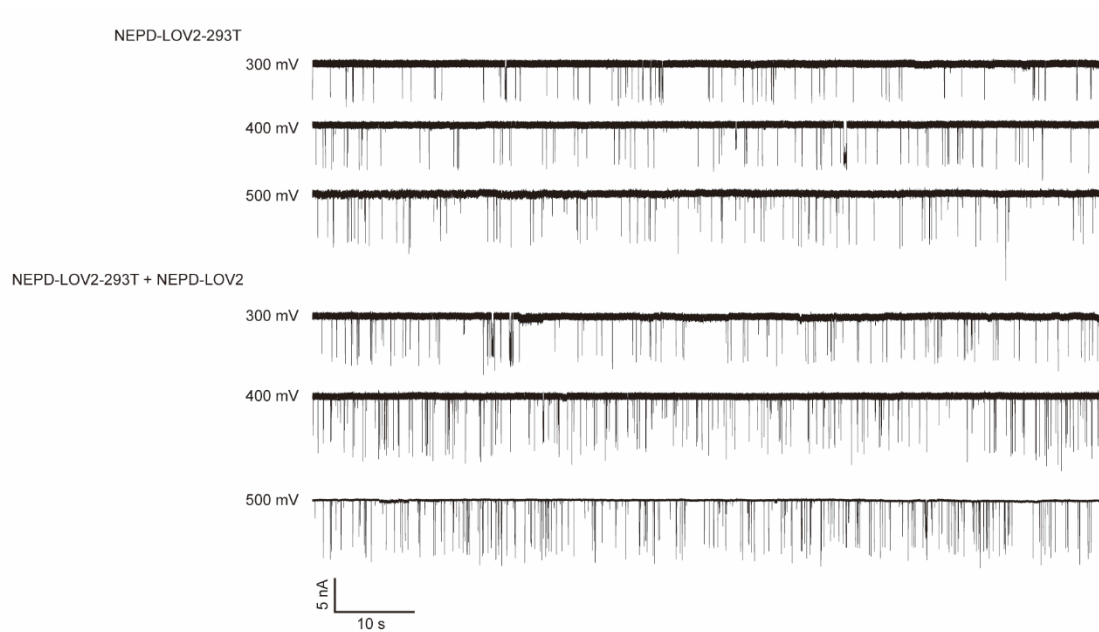


Figure S17. Additional raw current trace of NEPD-LOV2-293T and NEPD-LOV2-293T + NEPD-LOV2 with light condition in fig 4. The raw current trace of NEPD-293T under illumination conditions at 300mV, 400mV and 500mV voltage, using 9nm-in-diameter solid-state nanopore. The raw current trace of NEPD-293T + NEPD at 300mV, 400mV and 500mV voltage, using 9 nm-in-diameter solid-state nanopore.